J Solid State Electrochem (2002) 6: 272–278
DOI 10.1007/s100080100215

ORIGINAL PAPER

**Mirtat Bouroushian · Tatjana Kosanovic · Zafiris Loizos
Nicholas Spyrellis**

Electrochemical formation of zinc selenide from acidic aqueous solutions

Received: 10 November 2000 / Accepted: 15 March 2001 / Published online: 21 June 2001

Abstract An investigation on electrochemical ZnSe thin film growth from acidic aqueous baths of Se(IV) and Zn(II) species is described. The range of co-deposition potentials is predicted on a thermodynamic basis according to a known electrochemical model. A study on the voltammetric behavior of Ti and Ni electrode substrates in the working solutions at various temperatures provides the main features of the applied electrochemical process. Cathodic electrodeposition at high temperatures (> 65 °C) results in the formation of polycrystalline cubic, randomly oriented, ZnSe crystallites suffering, in general, from the presence of a crystalline Se phase in excess. Annealing of as-grown films adjusts the stoichiometry and leads to the production of semiconductive ZnSe with a band gap width of 2.7 eV.

Keywords Zinc selenide · Cathodic electrodeposition · Binary compound semiconductor · Underpotential deposition · Voltammetry

Introduction

Being a direct wide band gap semiconductor ($E_g = 2.7$ eV), zinc selenide exhibits great potential for various optoelectronic and high-speed applications like blue-green light emitting diodes, photoluminescent and electroluminescent devices, lasers and thin film solar cells [1, 2].

Polycrystalline ZnSe films, suitable for use as window layers in heterojunction solar cells, have been grown by various vacuum evaporation techniques (e.g. [1]), while molecular beam epitaxis and metalloorganic chemical vapor deposition have been used for the preparation of high-quality single-crystal ZnSe layers on GaAs [3] and related substrates. Low-temperature, relatively inexpensive, chemical solution growth procedures, offering the possibility of large area deposition, have been also used for the formation of the compound [2, 4, 5]; however, they result in the production of microcrystalline films. Hitherto, electrodeposition and related methods are far from being successful in efficient, polycrystalline ZnSe preparation, though their vital advantages such as simplicity and controllability substantiate the continuous investigation in the field. Reports on doped or undoped binary compound or ternary CdZnSe and HgZnSe film formation, in a potentio- or galvanostatic or even pulse-plating mode, have been published [6, 7, 8, 9, 10, 11, 12].

Electrosynthesis has proved to be very useful in the preparation of technologically important metal alloys, whereas the successful application in the formation of semiconductor alloys is more limited in range. It is commonplace that semiconductive binary compounds of well-defined stoichiometry can be prepared by underpotential deposition (u.p.d.) of the less noble element, induced by the free energy gained by compound's formation. In fact, the relevant electrochemical models providing valid predictions as to the equilibrium potentials of electrodeposited compounds have been the starting points for efficient thin film deposition (CdSe, CdTe) [13, 14, 15, 16].

The present work constitutes a study on an electrochemical method of ZnSe formation. After a brief analysis of the Zn-Se compound deposition thermodynamics, we investigate the voltammetric features of selenite using Ti and Ni electrodes in an excess of acidic aqueous zinc sulfate solution. Further, we report on the influence of plating conditions, such us bath composition and temperature, as well as on the effect of a post-annealing procedure, on the crystallinity, composition and semiconducting properties of the as-prepared films.

M. Bouroushian (✉) · T. Kosanovic · Z. Loizos · N. Spyrellis
General Chemistry Laboratory,
Chemical Engineering Department,
National Technical University of Athens,
Zografos Campus, 157 80 Athens, Greece
E-mail: mirtatb@central.ntua.gr
Tel.: +30-1-7723130
Fax: +30-1-7723088

Experimental

Voltammetry experiments were conducted in a thermostat-controlled, conventional three-electrode cell, with a potentio-scan (Wenking PGS 81R) system coupled to an X-Y recorder (HIOKI 8801 Memory Hi Corder). A rotating disc electrode system was used in order to control the mass transfer regime in the electrolytic solution. Working electrodes (WE) were commercially pure Ni and Ti discs of ~1.13 cm^2 geometrical area and the counter electrode was a large platinum grid. All reported potentials are referred to a commercial Hg/Hg_2SO_4 saturated sulfate reference (SSE). There was no correction for ohmic drop.

Water (of 18.3 MΩ cm), purified by an ultra-pure water system (Easy Pure Barnstead RF), and as-received analytical grade selenite (SeO_2) and $ZnSO_4.7H_2O$ reagents were used for the preparation of experimental solutions. Potassium sulfate was used in certain cases as a supporting electrolyte. The bath pH was adjusted by sulfuric acid at the working temperatures.

The preparation of reproducible Ni and Ti electrode surfaces included abrasion, polishing by 0.3 μm alumina powder and ultrasonic cleaning in ethanol and water. Prior to each deposition, Ti was chemically etched by 10% HF acid, for 10 s, in order to dissolve the surface oxide layer.

Thin films were obtained by cathodic electrodeposition under potentiostatic, mainly, as well as galvanostatic conditions for various plating times (corresponding to 0.5–5 C electrolysis charge). Several samples were submitted to annealing in a furnace controlled by a Shimaden FP21 programmable controller. Heating was carried out at a 10 °C/min rate up to 200 °C (in air) or higher, up to 700 °C (in an inert argon atmosphere in order to avoid the oxidation of Zn), and maintained for 15 min to 1 h. The structure of the as-prepared samples was examined by X-ray diffraction (XRD) by a Siemens D5000 unit. Scanning electron microscopy (SEM) images were taken by a JEOL JSM 6100 apparatus while band gap widths (E_g) were evaluated from reflectance spectra obtained by a Hitachi U-4001 spectrophotometer equipped with an integrating sphere. Compositional data were obtained by energy dispersive X-ray (EDX) local analysis during electron microscopy.

Thermodynamics of the binary compound deposition

In accordance with considerations applied to other II-VI compounds [14, 15, 17], a simple mechanism for ZnSe cathodic electro-forming as a result of Se(IV) and Zn^{2+} species co-reduction in an acidic environment is presumed:

$$H_2SeO_3 + 4e^- + 4H^+ \rightleftharpoons Se^0(s) + 3H_2O(E^\circ = +0.740V) \quad (1)$$

$$Zn^{2+} + 2e^- \rightleftharpoons Zn(s)(E^\circ = -0.763V) \quad (2)$$

$$Zn(s) + Se(s) \rightleftharpoons ZnSe(s) - 137\,kJ/mol(= \Delta G_{298K}[13]) \quad (3)$$

The relation between the activities of Zn and Se in ZnSe can be determined through reaction 3. Thermodynamically, the boundaries confining the existence range of the compound in a phase diagram denote the co-existence of a pure Se phase at one side (Se/ZnSe) and a pure Zn phase at the other side (ZnSe/Zn), where the activities of the discrete elements obtain their limiting values. The variations of Se and Zn activities over the existence range of ZnSe give rise to a corresponding change in the equilibrium potentials of the particular elements, which might be calculated by thermodynamic considerations.

Referring to the analytical derivations given in [13] (also [17] for a detailed analysis on CdSe), it can be estimated that the total variation of Zn equilibrium potential (E_{Zn}), with respect to the element's activity decrease from the ZnSe/Zn to Se/ZnSe phase boundaries, is equal to +0.709 V. Hence, Zn can be deposited at more positive potentials than its normal equilibrium value; that is, Zn can be deposited underpotentially. The complex character of selenium electrochemistry constrains the capability of deriving valid expressions for the Nernst reduction potentials of the Se(IV) species involved [17, 18, 19]; however, what interests us here is that, since the difference between Zn and Se standard potentials, $\Delta E^\circ = 0.74 - (-0.76) = 1.50$ V, is larger than the shift in the potential of the less noble element, $|\Delta E_{Zn}| = 0.709$ V, zinc is the potential-determining species in the whole range of electrolysis conditions. Thus, it is calculated that at 25 °C, for $[Zn^{2+}] = 0.2$ mol/L, independently of pH:

$$E_{ZnSe} = E_{Zn} = -0.71\,V/SSE \quad (4)$$

at Se/ZnSe and:

$$E_{ZnSe} = E_{Zn} = -1.42\,V/SSE$$

at ZnSe/Zn boundaries.

The increase of zinc ion concentration shifts the ZnSe deposition potentials at more positive values. For example, if $[Zn^{2+}] = 0.4$ mol/L, the potential range is estimated to be –0.66 to –1.36 V/SSE. Furthermore, higher temperatures, though moderately decrease the free energy increment of the ZnSe formation reaction, result in a similar anodic shift, through their effect on Nernst potentials. Note also that the above values may be changed by addition of overvoltage-containing terms of discharge overpotential and ohmic drop between the cathode contact and the reference electrode.

Provided that a large excess of Zn ions is present in the electrolytic solution, the above model suggests that a simultaneous reduction of Zn(II) and Se(IV) leading to the formation of ZnSe compound within the u.p.d. region of zinc is thermodynamically possible. The production of a stoichiometric compound may be achieved with a proper adjustment of mass transfer in solution towards the cathode, ensuring a 1:1 Zn/Se species reduction [13, 14, 15, 16]. However, complications in the preceding ideal description may be involved on account of side reactions such as H_2Se production and subsequent precipitation of ZnSe and Se species [8, 9, 19], hydrogen evolution, substrate influence and related phenomena [20, 21]. The following investigation within a wide range of experimental conditions may prove whether the formation of semiconductive ZnSe is possible as described.

Results

Voltammograms obtained from an excess of Zn^{2+} in acidic solutions of selenite can provide basic information about the process under investigation. Figure 1 contains cathodic polarization sweeps of Ti working electrodes in plating solutions at various temperatures, while the diagrams in Figs. 2 and 3 include the partial contributions of the electroactive species on cathodic current, for Ti and Ni electrodes at two different temperatures.

According to the plots in Figs. 2 and 3, obtained at a slow scan rate (5 mV/s), and hence approximately steady-state conditions, zinc bulk reduction from its precursor solution begins shortly after –1.5 V/SSE at 25 °C, and almost 0.1 V more positive at 85 °C. In the presence of Se(IV), the bulk metal reduction is shifted at slightly more negative values owing to the introduction of a nucleation overpotential.

At ambient temperatures and for a Ti cathode, the observed current at potentials positive to zinc deposition is wholly due to oxygen reduction in the bath (Fig. 2). Higher temperatures (85 °C) promote the Se(IV) reduction ("Se" curve) while, in the presence of excessive Zn^{2+}, a Se species diffusion-controlled regime appears to be established ("Zn + Se" curve). This is valid within the narrow range of equal or lower than 0.5×10^{-3} concentrations of Se precursor. A higher content results in the establishment of a Se(IV) reduction-controlled process (Fig. 4).

The WE rotation-rate dependence of cathodic current, within the nearly potential independent plateau region of Fig. 2 at 85 °C, lies in accordance with Levich's equation (Fig. 5; Ti), while the non-zero intercept of the straight line indicates that the deposition current is a fraction of its diffusion-limited value. Thereby, in the range of low Se concentrations employed, the process is controlled partially by convective diffusion of Se(IV) ions towards the cathode and partially by another process which, possibly, consists of slow adsorption/nucleation surface phenomena. Large deviations from linearity occur with Levich plots obtained at 65 °C and lower temperatures. Hence, convective diffusion becomes important when the temperature rises, while, at the same time, the overpotential in Zn bulk reduction on the Se-rich cathode progressively decreases (Fig. 1).

The behavior of the working-solutions/Ni-cathode system is not consistent with a diffusion-controlled process within the whole experimental condition range (e.g. Fig. 5; Ni at –1.4 V/SSE). The lower overpotential in hydrogen evolution and larger electroactivity complicate the situation in this case (Fig. 3) and generally induce a lower reproducibility in voltammetry compared with Ti. Even at ambient temperatures, a selenite-containing solution depolarizes the Ni cathode soon after the onset of the potential scan ("Se" curve), while, in the presence of excessive zinc, the reduction of Se(IV) and H^+ is suppressed by metal ions present in the diffusion layer and adsorbed at the cathodic surface ("Zn + Se" curve). In the absence of Se, a cathodic peak preceding the zinc deposition wave is clearly observed at about –1.3 V/SSE at all temperatures ("Zn" curve). The existence of this "prewave" is associated with hydrogen evolution inhibited by zinc ion adsorption, as being a diminished form of the "blank" curve (note that the larger overpotential of hydrogen on Ti precludes the occurrence of such a peak). It has been suggested (though with aluminum alloy cathodes in zinc sulfate

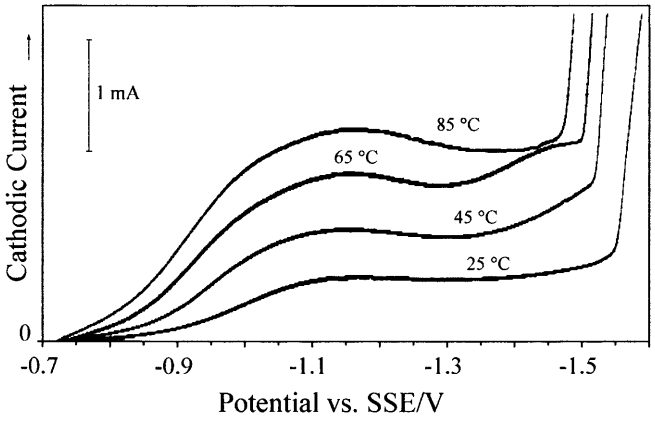

Fig. 1 Ti cathodic polarization curves at a 5 mV/s scan rate in a 0.5×10^3 M SeO_2, 0.2 M $ZnSO_4$, pH 2.5 solution for various bath temperatures (rotation rate: 500 rpm)

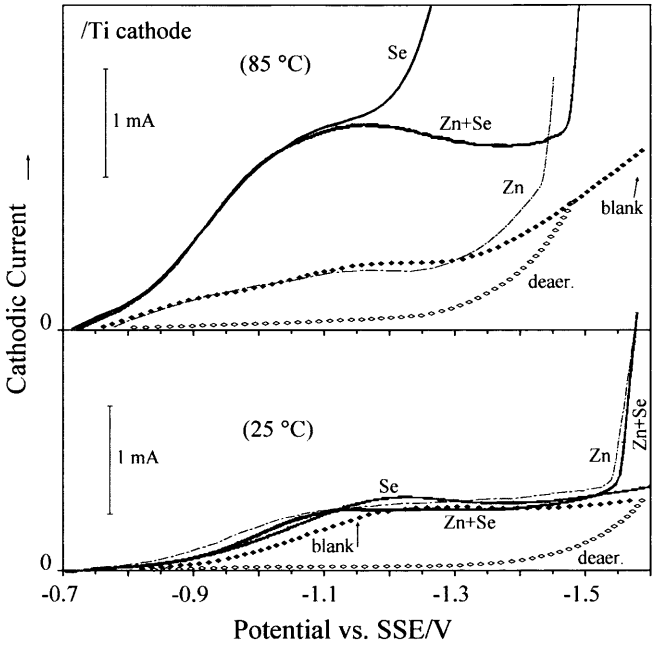

Fig. 2 Cathodic polarization of Ti electrode at a 5 mV/s scan rate (rotation rate: 500 rpm) at various bath compositions and temperatures. Partial "blank" curves show acidic (pH 2.5) 0.2 M K_2SO_4 solutions; "deaer." is a deaerated blank solution; "Se" and "Zn" curves show 0.5×10^{-3} M SeO_2, 0.2 M K_2SO_4 and 0.2 M $ZnSO_4$, acidic (pH 2.5) solutions, respectively; "Zn + Se" curves concern 0.5×10^{-3} M SeO_2, 0.2 M $ZnSO_4$, acidic solutions

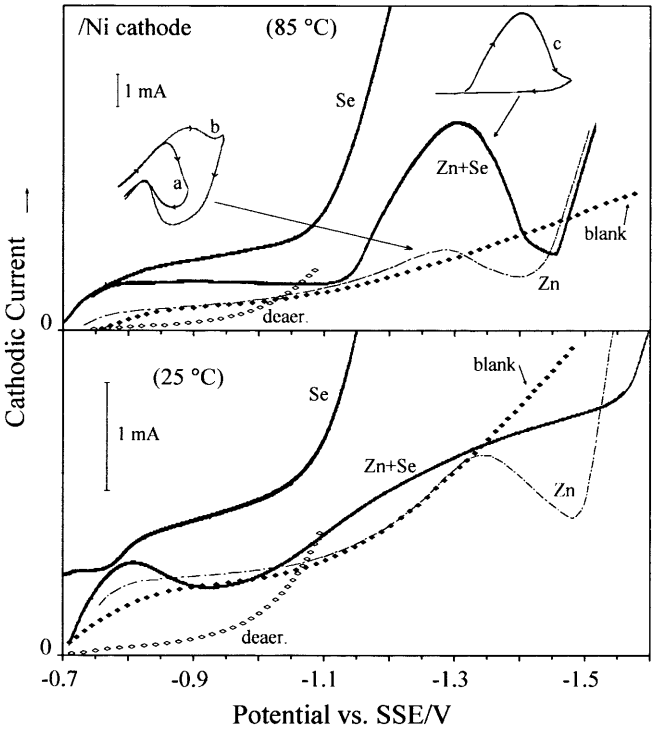

Fig. 3 Cathodic polarization of Ni electrode at a 5 mV/s scan rate (rotation rate: 500 rpm) (see legend of Fig. 2 for notation). Reversal of the polarization sweep at the right foot of the "prewave" at "Zn" curve gives an anodically directed reverse wave. Further analysis by cyclic sweeps at various scan rates [e.g. (*a*) 50 mV/s; (*b*) 250 mV/s shown in the pattern] indicates that: (1) the cathodic peak current density is almost proportional to the square root of the scan rate over a wide range of scan rates (10–500 mV/s); (2) the cathodic peak potential shifts negatively with increasing scan rate; and (3) the difference between the cathodic and anodic peaks' potentials is low and slightly increasing with scan rate. The prewave at the "Zn + Se" curve is shown with a sweep reversal at –1.45 V/SSE (*c*)

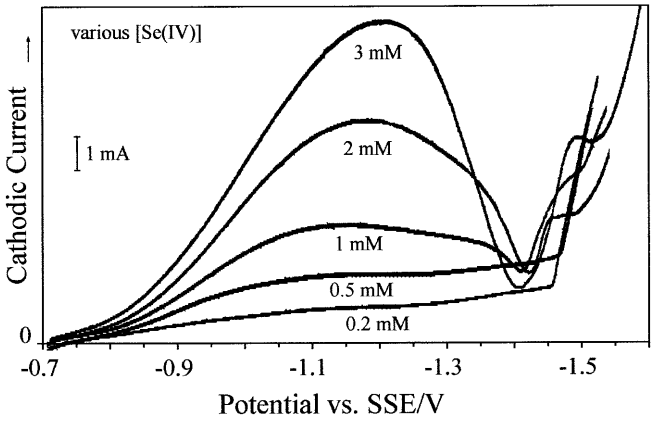

Fig. 4 Ti cathodic polarization curves at a 5 mV/s scan rate in a 0.2 M $ZnSO_4$, pH 2.5, solution for various SeO_2 concentrations [0.2, 0.5, 1, 2, 3 ($\times 10^{-3}$ M)]. Bath temperature: 85 °C

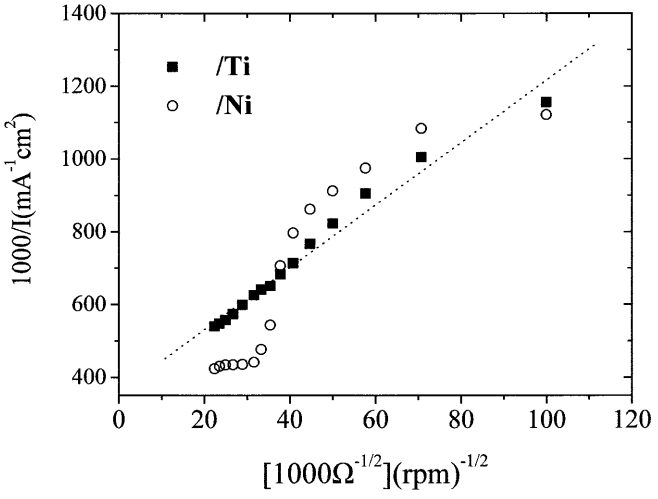

Fig. 5 Koutecky-Levich plots of I^{-1} vs. $\Omega^{-1/2}$ for Ti and Ni cathodes at a bath temperature of 85 °C. The working potentials lie in the "plateau" region (–1.2 V/SSE for Ti and –1.4 V/SSE for Ni electrodes)

solution [22, 23]) that this voltammetric behavior may involve also a charge transfer connected to zinc underdeposition. However, according to diagnostic tests on cyclic voltammograms at various scan rates (see legend of Fig. 3), the system is quasi-reversible and rather consistent with a simple effect of zinc ion adsorption/desorption.

The presence of selenite, along with Zn^{2+}, intensifies the prewave at 85 °C (Fig. 3, "Zn + Se" curve), certainly due to the addition of an increased Se reduction current but, possibly, as promoting also an electron transfer by zinc u.p.d., in agreement with the thermodynamic predictions. The prewave then represents an irreversible reduction, along with hydrogen evolution and ion adsorption (Fig. 3, curve c). The peak current decreases and finally disappears at higher scan rates (50, 100 mV/s), owing to changes in the complex kinetic and mass transport features of the relevant reactions. In any case, Zn co-deposition can be verified, since removal of elemental Se formed during cyclic polarization (by heating) leaves a thin yellowish layer of ZnSe on the electrode surface.

In general, examination of layers obtained on Ni and Ti indicate that Zn u.p.d. and formation of ZnSe occurs at potentials at least as anodic as –0.9 V/SSE, in full agreement with the thermodynamic predictions (taking overpotential into account).

According to XRD (Fig. 6), increase of the bath temperature promotes the formation of cubic blend ZnSe crystallites, exhibiting a random orientation. Together with the compound, a metallic, hexagonal Se phase is obtained at temperatures higher than 45 °C. At constant temperature and deposition potential, the Se to ZnSe mass ratio in the solid is rather independent of the layer thickness (Fig. 7), provided that the deposition of Se is partially controlled by diffusion of Se(IV) to the cathode (Ti substrate).

The Zn/Se atom ratio in a deposit depends on nucleation and growth conditions, including the substrate effect. Thus, a smooth Ni substrate seems to initially

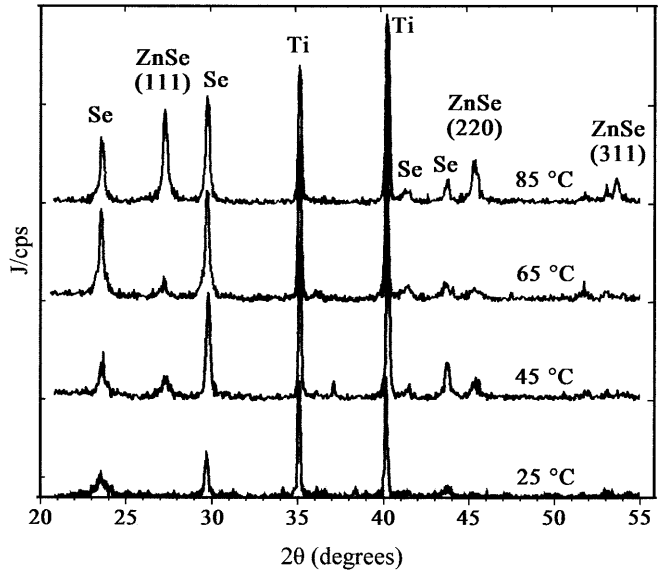

Fig. 6 XRD patterns (Cu K_α source) of equally thick deposits prepared on Ti at –1.2 V/SSE from a 0.5×10^{-3} M SeO_2, 0.2 M $ZnSO_4$, pH 2.5 solution at various temperatures (25–85 °C)

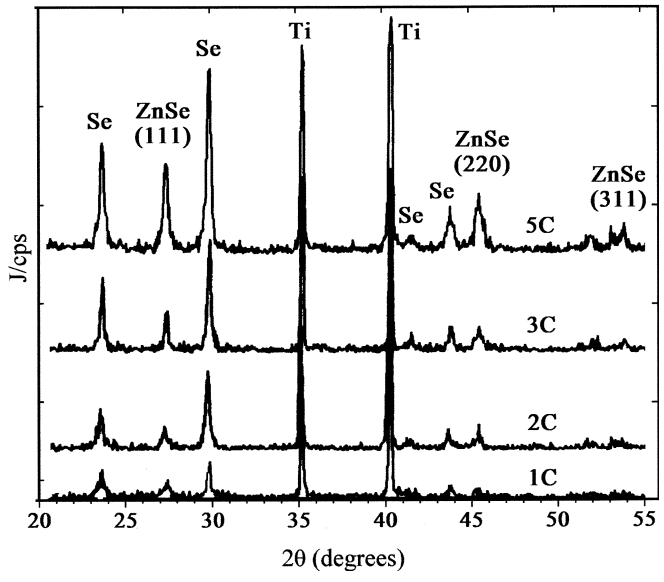

Fig. 7 XRD patterns (Cu K_α source) of deposits prepared on Ti at –1.2 V/SSE from a 0.5×10^{-3} M SeO_2, 0.2 M $ZnSO_4$, pH 3 solution at 85 °C for various plating charges (1–5 C)

induce a higher Zn/Se ratio, which decreases with the thickness of the layer (Fig. 8) as the absence of diffusion control promotes the copious deposition of Se. On the other hand, a homogeneously nucleated phase, often exclusively consisting of Se (Fig. 9a), may occur on the rough (due to chemical pretreatment; see above) titanium substrate during the first minutes of deposition; however, growth restores a Zn/Se = 0.1–0.6 ratio, depending approximately on the preparation conditions. Thus, according to EDX, for films deposited on Ti at –1.1 V to –1.3 V/SSE, the Zn content can reach 37 at%,

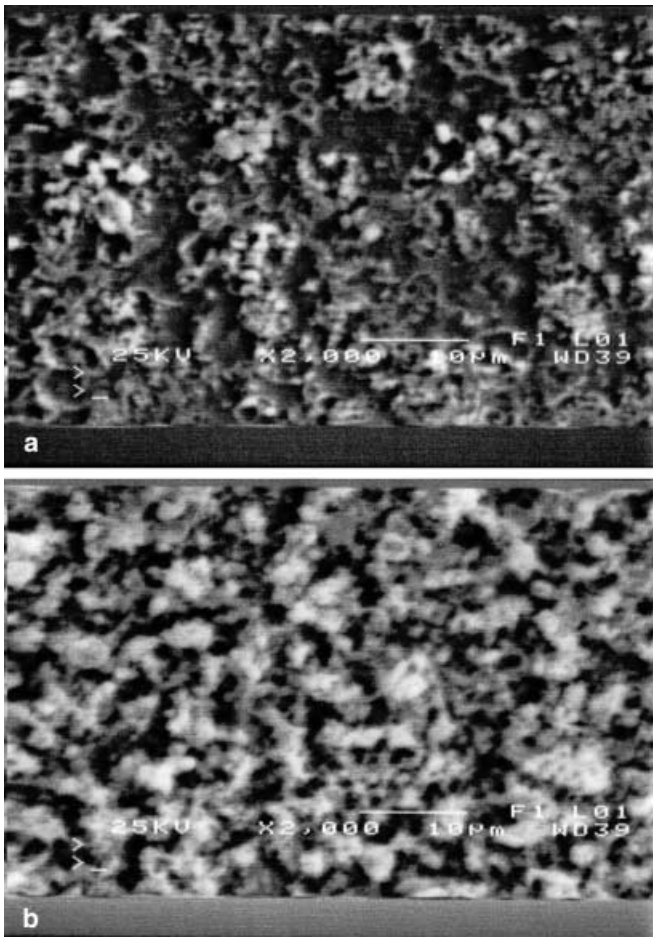

Fig. 8a, b SEM micrographs of deposits prepared on Ni at –1.3 V/SSE from a 0.5×10^{-3} M SeO_2, 0.2 M $ZnSO_4$, pH 3 solution at 85 °C. Plating charge is **a** 0.7 C and **b** 5 C. Average atomic composition from EDX: **a** 10.1% Zn, 89.9% Se; **b** 1.8% Zn, 98.2% Se. The *white regions* are Se-rich clusters (EDX: almost 95% Se)

although, usually, lies at about 20–30 at%. The selenium content is generally increased at –1.4 V/SSE. Deposits of similar thickness on Ni present higher contents of Se in the whole range of applied conditions, while hydrogen evolution decreases the current efficiency and results in flaking of the films; the impact of hydrogen bubbles is obvious in the micrograph of Fig. 8a.

A strict resumé of the results for Ti substrate is the following. Within the investigated range of bath pH 2.0–5.5 and $[Zn^{2+}] = 0.01$–0.8 M, at 85 °C (as an optimal choice to encounter with the instability of near boiling baths, though the latter often lead to better results), the potentiostatic deposition gave optimal results at the range: $E = -1.1$ to –1.3 V/SSE; bath pH = 2.5–4; $[SeO_2] \le 0.5\times10^{-3}$ M and $[Zn^{2+}] > 0.1$ M. The as-obtained films are grayish and moderately adherent to the substrate. Matching results can be obtained by applying galvanostatic deposition under similar conditions, at current densities in the range of 0.2–0.8 mA/cm^2.

The XRD patterns (Fig. 10A) of "good" samples show well-resolved ZnSe (111), (220) and (311) diffraction

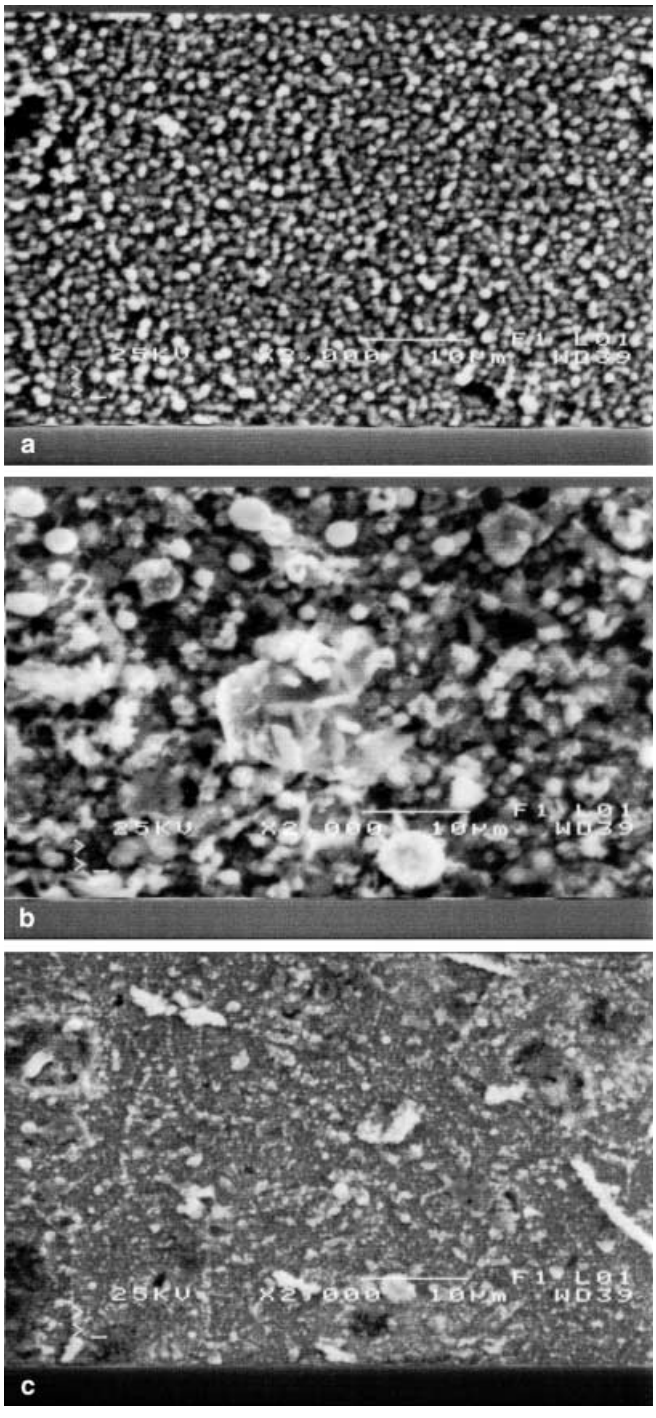

Fig. 9a–c SEM micrographs of deposits prepared on Ti at –1.2 V/SSE from a 0.5×10^{-3} M SeO_2, 0.2 M $ZnSO_4$, pH 3 solution at 85°C. As-deposited at a plating charge of **a** 0.5 C and **b** 5 C. Average atomic composition from EDX: **a** almost 100% Se; **b** 19.1% Zn, 80.9% Se (*white regions* are almost 95% Se). **c** The previous sample after heat treatment at 200 °C in air for 15 min; EDX: 47% Zn, 53% Se

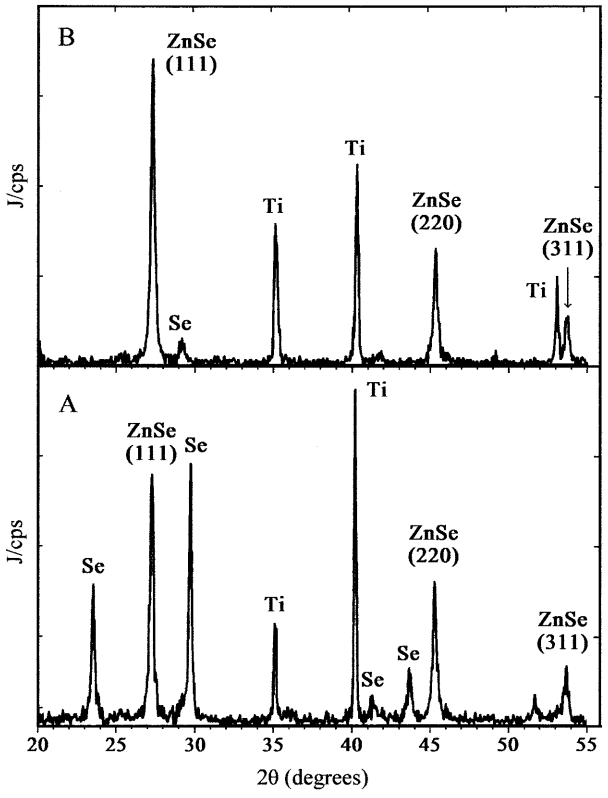

Fig. 10A, B XRD patterns (Cu K_α source) of a Zn-Se/Ti layer prepared at –1.2 V/SSE from a 0.2×10^{-3} M SeO_2, 0.2 M $ZnSO_4$, pH 3 solution at 85 °C. Before (**A**) and after annealing (**B**) at 200 °C in air for 30 min

peaks, indicating the existence of well-formed compound crystallites. Annealing at 200 °C in air or at higher temperatures in an inert atmosphere adjusts the stoichiometry, establishing a virtually 1:1 Zn/Se composition, as removing excessive Se by sublimation and/or evaporation (Fig. 10B). At temperatures higher than 450 °C a small deficiency of Se (2–3% according to SEM, i.e. a Zn/Se ratio increment to 1.1–1.2) is observed, as a portion of ZnSe is transformed to ZnO [24], owing to the presence of oxygen traces in the furnace. In general, thermal treatment gives rise to more cohesive films, which often exhibit the characteristic yellowish color of ZnSe; however, this has a minor effect on film crystallographic structure (Fig. 10B). Note that nearly amorphous (as-deposited) samples give a well-defined (111)-oriented ZnSe XRD response when annealed at high temperatures (700 °C), a phenomenon possibly related to the observed, parallel formation of a ZnO- zincite phase.

The SEM micrograph in Fig. 9b shows the large Se-rich clusters selectively grown under the poorly controlled deposition of a binary compound. The deposit, in general, constitutes an aggregate of spherical clusters which rather precipitate (possibly after a homogeneous reaction between Zn^{2+}, H_2SeO_3 and H_2Se formed in some distance of the cathode [8, 9, 19]) than grow after a planar superficial diffusion of reduced ad-atoms [21]). An annealing procedure leaves a more compact and adherent layer with a few Se-rich forms (Fig. 9c), which can be removed by further heating.

The removal of excessive Se from as-deposited layers is possible also with chemical etching. Thus, according to

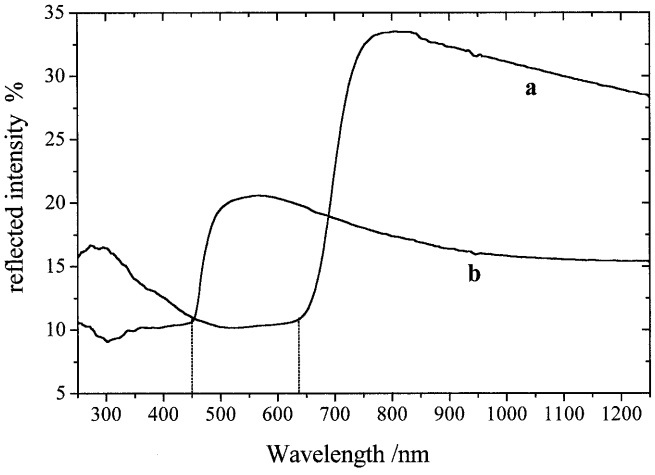

Fig. 11a, b Reflection spectra of a Zn-Se/Ti sample prepared at –1.3 V/SSE from a 0.5×10^{-3} M SeO_2, 0.8 M $ZnSO_4$, pH 2.5 solution at 85 °C. **a** As-deposited; **b** after heat treatment at 500 °C in Ar atmosphere for 1 h. Atomic composition from EDX: **a** 11.9% Zn, 88.1% Se; **b** 53% Zn, 47% Se. The estimated band gap widths are **a** 1.94 eV; **b** 2.7 eV

EDX, the immersion of samples in an alkaline polysulfide (1 M in Na_2S, S, NaOH) solution results in a sharp decrease of Se content and a complete change of appearance (gray color turns to the orange-yellow of ZnSe).

Spectroscopic analysis of totally reflected light, allowing the evaluation of the band gap energy of the deposited layers, proved that ZnSe exhibiting a well-defined semiconductive behavior can be obtained. Curve (a) in Fig. 11 shows the response of an as-deposited Se-rich, gray sample exhibiting a characteristic band gap width of crystalline, hexagonal Se (1.94 eV). The response of the same sample after removal of the excessive Se phase by annealing (b) corresponds to the characteristic transition of ZnSe with $E_g = 2.7$ eV.

Conclusions

It has been demonstrated that, according to thermodynamics considerations, the electrolytic synthesis of semiconductive ZnSe is theoretically possible from acidic solution within the underpotential range of zinc reduction. An experimental procedure was derived, resulting in the preparation of polycrystalline, cubic blend ZnSe of random orientation by electrodeposition on Ti and Ni electrodes from excess Zn(II) in acidic aqueous solutions of Se(IV).

In the frame of the applied method, a high bath temperature is essential in obtaining well-formed crystallites of the compound, while it is necessary to control the deposition potential, bath composition and substrate. Then, by appropriate adjustment of hydrodynamic conditions, the process is partially controlled by convective diffusion of Se(IV) ions towards the cathode. However, it is not possible to avoid the parallel formation of a selenium phase, as fairly cathodic deposition potentials are required owing to the reductive nature of zinc.

The deposition substrate nature plays a key role in dealing with hydrogen evolution within the applied potentials as well as in providing specific nucleation conditions, i.e. it influences the competition between nucleation of Se and ZnSe.

Annealing of Se-rich electrodeposits, even at 200 °C for a few minutes, adjusts the stoichiometry by removing the Se excess, yet hardly ameliorates the crystallinity of the compound. The as-annealed films show the characteristic transition of semiconductive ZnSe at 2.7 eV.

Acknowledgements The authors would like to thank Dr. George Maurin, Research Director of C.N.R.S. (Laboratory UPR 15, Physique des Liquides et Electrochimie), for helpful discussions and technical assistance.

References

1. Lakshmikumar ST, Rastogi AC (1995) Thin Solid Films 259:150
2. Lokhande CD, Patil PS, Tributsch H, Ennaoui A (1998) Solar Energy Mater Solar Cells 55:379
3. Franciosi A, Van de Walle CG (1996) Surf Sci Rep 25:1
4. Wang C, Qian XF, Zhang WX, Xie Y, Quian YT (1999) Mater Res Bull 34:1637
5. Dona JM, Herrero J (1995) J Electrochem Soc 142:764
6. Krishnan V, Ham D, Mishra KK, Rajeshwar K (1992) J Electrochem Soc 139:23
7. Rai JP, Singh K (1993) Indian J Chem A 32:376
8. Natarajan C, Sharon M, Levy-Clement C, Neumann-Spallart M, (1994) Thin Solid Films 237:118
9. Natarajan C, Sharon M, Levy-Clement C, Neumann-Spallart M, (1995) Thin Solid Films 257:46
10. Natarajan C, Nogami G, Sharon M (1995) Thin Solid Films 261:44
11. Samantilleke AP, Boyle MH, Young J, Dharmadasa IM (1998) J Mater Sci Mater Electron 9:231
12. Konigstein C, Ernst K, Spallart M (1998) In: Proceedings of the 10th workshop on quantum solar energy conversion (Quantsol'98), Bad Hofgastein, Austria
13. Kröger FA (1978) J Electrochem Soc 125:2028
14. Panicker P, Kröger FA, Castner M (1978) J Electrochem Soc 125:566
15. Loizos Z, Spyrellis N, Maurin G, Pottier D (1989) J Electroanal Chem 269:399
16. Bouroushian M, Loizos Z, Spyrellis N, Maurin G (1993) Thin Solid Films 229:101
17. Bouroushian M, Kosanovic T, Loizos Z, Spyrellis N (2000) Electrochem Commun 2:281
18. Zhdanov SI (1974) Selenium. In: Bard AJ (ed) Encyclopedia of electrochemistry of the elements, vol IV. Dekker, New York, pp 361–392
19. Zuman P, Somer G (2000) Talanta 51:645
20. Bouroushian M, Loizos Z, Spyrellis N (2000) Appl Surf Sci 156:125
21. Cachet H, Cortes R, Froment M, Maurin G (1997) J Solid State Electrochem 1:100
22. Ettelm VA (1984) Interpretation of polarization measurements in zinc electrolytes. In: Warren IH (ed) Application of polarization measurements in the control of metal deposition. (Process metallurgy 3) Elsevier, Amsterdam, pp 32–46
23. Fosnacht DR, O'Keefe TJ (1980) J Appl Electrochem 10:495
24. Chaparro AM, Martinez MA, Guillen C, Bayon R, Gutierrez MT, Herrero J (2000) Thin Solid Films 361–362:177